Triplet-singlet relaxation in semiconductor single and double quantum dots

K. Shen[1] and M. W. Wu[1,2,*]

[1]*Hefei National Laboratory for Physical Sciences at Microscale, University of Science and Technology of China, Hefei, Anhui 230026, China*

[2]*Department of Physics, University of Science and Technology of China, Hefei, Anhui 230026, China*

(Received 20 August 2007; published 17 December 2007)

We study the triplet-singlet relaxation in two-electron semiconductor quantum dots. Both single dots and vertically coupled double dots are discussed. In our work, the electron-electron Coulomb interaction, which plays an important role in the electronic structure, is included. The spin mixing is caused by spin-orbit coupling which is the key to the triplet-singlet relaxation. We show that the selection rule widely used in the literature is incorrect unless near the crossing and/or anticrossing point in single quantum dots. The triplet-singlet relaxation in double quantum dots can be markedly changed by varying barrier height, interdot distance, external magnetic field, and dot size.

DOI: 10.1103/PhysRevB.76.235313 PACS number(s): 73.21.La, 71.70.Ej, 72.10.Di, 73.22.Lp

I. INTRODUCTION

The application of semiconductor quantum dots (QDs) in generating spin-based qubits[1,2] is one of the focuses in the field of spintronics.[3] There are two types of qubits investigated extensively recently.[2] One is based on the transition between single-electron Zeeman sublevels[4,5] and the other is based on two-electron triplet-singlet (TS) states.[6–11] Among these works, the decoherence time of the spin states, including both the spin dephasing time[7,8] and spin relaxation time,[5,9–11] has attracted much attention as a thorough understanding of it is one of the prerequisites of the application. There are many works on spin relaxation reported, especially in single-electron QDs.[12–23] Recently, the TS relaxation time of two-electron system has also been investigated.[24–27] It was proposed that various mechanisms, such as the electron-phonon scattering together with the spin-orbit coupling,[28,29] the hyperfine interaction,[30,31] and the cotunneling effect, could induce TS relaxation.[24] However, the mechanism involving electron-phonon scattering is usually treated as the key because the nuclei-mediated relaxation[32] and the cotunneling can be weakened via tuning external magnetic field and tunneling rates,[10] respectively.[24] Specifically, Climente *et al.* used exact diagonalization technique to calculate the two-electron spectrum structure and the phonon induced TS relaxation in parabolic single QDs.[24] They demonstrated the crucial role of the excited states on spectrum structure and showed a slow decrease of the relaxation time away from the TS crossing in contrast to a sharp increase in the vicinity of the crossing point, when the magnetic field is increased from 0 T. This feature agrees qualitatively with the recent measurement.[11] Furthermore, their results indicated that the spin-down triplet state coupled with the singlet ground state through the spin-orbit coupling has a much shorter lifetime compared to the other two triplet states. This was understood by the so called "selection rule" based on the perturbation using the lowest two single-electron levels. Similar perturbative discussion was also given in Ref. 25. Meunier *et al.* obtained perturbative wave functions from the selection rule and treated the spin-orbit coupling coefficient as a fitting parameter.[11] Using these functions, they fitted their experiment a data with electron-phonon scattering-induced TS relaxation and obtained a particularly small spin-orbit coupling coefficient. They attributed the reduction of the coupling coefficient to the neglect of high excited states. Sasaki *et al.* pointed out that the selection rule was correct only in the vicinity of the TS crossing point,[10] which seems to be more correct intuitively. According to the previous work by one of the authors[14] and confirmed by Destefani and Ulloa,[17] the spin-orbit coupling in quantum dots is very strong and a large number of basis functions are needed in order to achieve convergence even for the lowest few states. Therefore, whether the selection rule based on the lowest few levels remains unchanged when many upper levels are involved remains questionable to us. Therefore, in this work we will first reinvestigate the selection rule based on exact diagonalization method, jointly with perturbation method with many basis functions.

The investigation on TS relaxation in double QD architectures is very limited. Recently, Wang and Wu studied the single-electron spin relaxation in vertically coupled double QDs and showed that the spin relaxation can be efficiently manipulated electronically by the interdot barrier.[20] This suggests that the two-electron TS relaxation should also be manipulated by tuning interdot barrier height. This is another issue we are going to explore in this work.

We organize the paper as follows: In Sec. II we set up the model and lay out the formalism. Then in Sec. III we show our numerical results. We discuss the single dot case in Sec. III A. We first show the exact diagonalization results with sufficient basis functions. We then reexamine the selection rule by using more basis functions instead of the lowest two, both perturbatively and exactly. We show that the selection rule widely used in the literature is not correct except near the TS crossing and/or anticrossing points. In Sec. III B, we show the results of double QDs. We summarize in Sec. IV.

II. MODEL AND FORMALISM

We start our investigation from a vertically coupled double QD: Electrons are confined by a parabolic potential $V_c(x,y)=\frac{1}{2}m^*\omega_0^2(x^2+y^2)$ (corresponding to the effective dot

diameter $d_0=\sqrt{\hbar\pi/m^*\omega_0}$) along the x-y plane,[33,34] with m^* representing the effective mass. Along the z axis, a strong confinement is given by

$$V_z(z)=\begin{cases} V_0, & |z|\leqslant \frac{1}{2}a \\ 0, & \frac{1}{2}a<|z|<\frac{1}{2}a+d \\ \infty & \text{otherwise}, \end{cases} \tag{1}$$

with V_0, the interdot barrier.[35] By taking $a=0$, one comes to the single dot configuration. The single-electron Hamiltonian with magnetic field along the growth direction (z) is given by

$$H_e=\frac{\mathbf{P}^2}{2m^*}+V(\mathbf{r})+H_{so}(\mathbf{P})+H_Z, \tag{2}$$

in which $V(\mathbf{r})=V_z(z)+V_c(x,y)$ and $\mathbf{P}=-i\hbar\nabla+e/c\mathbf{A}$ with $\mathbf{A}=(B/2)(-y,x,0)$. H_{so} represents the spin-orbit coupling which is the key to the spin flip. In this work, we only consider the Dresselhaus spin-orbit coupling[28] as the Rashba coupling[29] is comparably small in GaAs QDs.[36] Hence $H_{so}=\gamma\mathbf{h}\cdot\sigma$, with $\mathbf{h}=[P_x(P_y^2-P_z^2),P_y(P_z^2-P_x^2),P_z(P_x^2-P_y^2)]$.[37] For small well width, it reduces to

$$H_{so}=\frac{\gamma}{\hbar^3}\langle P_z^2\rangle(-P_x\sigma_x+P_y\sigma_y), \tag{3}$$

with $\langle P_z^2\rangle$ the average of P_z^2 over the electronic states defined by $V_z(z)$. $H_Z=\frac{1}{2}g\mu_B B\sigma_z$ is the Zeeman splitting with g being the Landé factor. We define $H_0=\frac{\mathbf{P}^2}{2m^*}+V(\mathbf{r})$, whose eigenvalues and eigenfunctions can be obtained from the Schrödinger equation

$$H_0|\phi\rangle=E|\phi\rangle. \tag{4}$$

Previous work on single-electron QDs gives the solution of the lateral part of this equation,[14,33,34] where the exact energy levels are given by

$$E_{nl}=\hbar\Omega(2n+|l|+1)+\hbar l\omega_B, \tag{5}$$

with $\Omega=\sqrt{\omega_0^2+\omega_B^2}$ and $\omega_B=eB/(2m^*)$. The wave functions read

$$\langle\mathbf{r}|nl\rangle=N_{n,l}(\alpha r)^{|l|}e^{-(\alpha r)^2/2}L_n^{|l|}((\alpha r)^2)e^{il\theta}, \tag{6}$$

with $N_{n,l}=(\alpha^2 n!/\pi(n+|l|)!)^{1/2}$ and $\alpha=\sqrt{m^*\Omega/\hbar}$. $L_n^{|l|}$ is the generalized Laguerre polynomial. In these equations, $n=0,1,2,\ldots$ is the radial quantum number and $l=0,\pm1,\pm2,\ldots$ is the azimuthal angular momentum quantum number. By solving the z component of Eq. (4), we obtain the lowest two electronic states along the z axis as follows:

$$\phi_z^0=\begin{cases} C_1^0\sin\left[k\left(z-\frac{a}{2}-d\right)\right], & \frac{a}{2}<z<\frac{a}{2}+d \\ C_2^0\cosh(\beta z), & |z|\leqslant\frac{1}{2}a \\ C_1^0\sin\left[k\left(-z-\frac{a}{2}-d\right)\right], & -\frac{a}{2}-d<z<-\frac{a}{2} \end{cases} \tag{7}$$

and

$$\phi_z^1=\begin{cases} C_1^1\sin\left[k\left(z-\frac{a}{2}-d\right)\right], & \frac{a}{2}<z<\frac{a}{2}+d \\ C_2^1\sinh(\beta z), & |z|\leqslant\frac{1}{2}a \\ C_1^1\sin\left[k\left(z+\frac{a}{2}+d\right)\right], & -\frac{a}{2}-d<z<-\frac{a}{2}, \end{cases} \tag{8}$$

in which $k^2=2m^*E_z/\hbar^2$ and $\beta^2=2m^*(V_0-E_z)/\hbar^2$ with E_z denoting the energy along this direction. We use the superscripts "0" and "1" to denote the even and odd parities, respectively. The total spatial wave function is then denoted by $|nln_z\rangle$, with $n_z=0$ and 1 in this work to distinguish the above even and odd states along the z axis. Due to the strong confinement along the z axis, levels higher than $n_z=1$ are neglected. It is noted that when we refer to the single QDs, we only keep the lowest state (the even one) due to the small well width.

For two-electron system, the total Hamiltonian is written as

$$H_{tot}=(H_e^1+H_e^2+H_C)+H_{ep}^1+H_{ep}^2+H_p. \tag{9}$$

In this equation, the third term $H_C=\frac{e^2}{4\pi\epsilon_0\kappa|\mathbf{r}_1-\mathbf{r}_2|}$ describes the Coulomb interaction between the two electrons with κ representing the static dielectric constant. $H_p=\Sigma_{\mathbf{q}\lambda}\hbar\omega_{\mathbf{q}\lambda}a_{\mathbf{q}\lambda}^+a_{\mathbf{q}\lambda}$ represents the phonon Hamiltonian, and $H_{ep}=\Sigma_{\mathbf{q}\lambda}M_{\mathbf{q}\lambda}(a_{\mathbf{q}\lambda}^+ +a_{\mathbf{q}\lambda})\exp(i\mathbf{q}\cdot\mathbf{r})$ is the Hamiltonian of the electron-phonon interaction. The superscripts "1" and "2" label the two electrons.

We construct two-electron basis functions from the single-electron wave functions. To see the physics clearly, we construct our two-electron basis functions in either singlet or triplet forms. Taking two single-electron spatial wave functions $|n_1l_1n_{z1}\rangle$ and $|n_2l_2n_{z2}\rangle$ (denoted as $|N_1\rangle$ and $|N_2\rangle$ for short) as an example, the singlet functions can be constructed by

$$|S\rangle=(|\uparrow\downarrow\rangle-|\downarrow\uparrow\rangle)\otimes\begin{cases}\frac{1}{\sqrt{2}}|N_1N_2\rangle, & N_1=N_2 \\ \frac{1}{2}(|N_1N_2\rangle+|N_2N_1\rangle), & N_1\neq N_2,\end{cases} \tag{10}$$

and the triplet functions for $N_1\neq N_2$ by

$$|T_+\rangle=\tfrac{1}{\sqrt{2}}(|N_1N_2\rangle-|N_2N_1\rangle)\otimes|\uparrow\uparrow\rangle, \tag{11}$$

$$|T_0\rangle = \tfrac{1}{2}(|N_1N_2\rangle - |N_2N_1\rangle) \otimes (|\uparrow\downarrow\rangle + |\downarrow\uparrow\rangle), \tag{12}$$

$$|T_-\rangle = \tfrac{1}{\sqrt{2}}(|N_1N_2\rangle - |N_2N_1\rangle) \otimes |\downarrow\downarrow\rangle. \tag{13}$$

Here, N and N', in the ket $|NN'\rangle$, represent the spatial quantum numbers of the first and the second electrons, respectively. We define the total angular momentum $L=l_1+l_2$ and denote the total spin (S,S_z) with S_z representing the z component of the total spin $\mathbf{S}$.

Then, we calculate the matrix elements of the Coulomb interaction and the spin-orbit coupling[14] under these basis functions. The Coulomb matrix elements can be expressed in the form

$$\langle N_1N_2|H_C|N_1'N_2'\rangle = \frac{e^2}{4\pi^2\epsilon_0\kappa}\delta_{l_{N_1}+l_{N_2},l_{N_1'}+l_{N_2'}}Q(N_1,N_2,N_1',N_2'), \tag{14}$$

in which Q is given in detail in the Appendix. Thus we obtain the two-electron Hamiltonian. By diagonalizing the two-electron Hamiltonian, one obtains all the energy levels and eigenfuctions. We identify a state as singlet and/or triplet if its amplitude of singlet and/or triplet components is larger than 50%. We rewrite the spin-orbit coupling Hamiltonian [Eq. (3)] using the ladder operators as[24]

$$H_{so} = \gamma_c(P^+S^+ + P^-S^-), \tag{15}$$

with the coupling coefficient $\gamma_c = \frac{\gamma}{\hbar^3}\langle P_z^2\rangle$. Then it is noted that $P^\pm$ and $S^\pm$ change L and S_z by one unit, respectively. It suggests that a state with (L,S_z) can only be coupled with the states with $(L+1,S_z+1)$ and $(L-1,S_z-1)$.

Treating $|i\rangle$ and $|f\rangle$ as the initial and final states, we can calculate the phonon-induced relaxation rate from the Fermi golden rule

$$\Gamma_{i\to f} = \frac{2\pi}{\hbar}\sum_{\mathbf{q}\lambda}|M_{\mathbf{q}\lambda}|^2|\langle f|\chi|i\rangle|^2[\bar{n}_{\mathbf{q}\lambda}\delta(\epsilon_f-\epsilon_i-\hbar\omega_{\mathbf{q}\lambda}) + (\bar{n}_{\mathbf{q}\lambda}+1)\delta(\epsilon_f-\epsilon_i+\hbar\omega_{\mathbf{q}\lambda})], \tag{16}$$

in which $\chi(\mathbf{q},\mathbf{r}_1,\mathbf{r}_2)=e^{i\mathbf{q}\cdot\mathbf{r}_1}+e^{i\mathbf{q}\cdot\mathbf{r}_2}$ comes from the total electron-phonon interaction Hamiltonian $H_{ep}=H_{ep}^1+H_{ep}^2$. Here, $\bar{n}_{\mathbf{q}\lambda}$ represents the Bose distribution of phonon with mode λ and momentum $\mathbf{q}$. In our calculation, the temperature is fixed at 0 K. Therefore only the phonon emission process occurs.

III. NUMERICAL RESULTS

In the numerical calculation, we include the electron-acoustic phonon scattering due to the deformation potential with $|M_{\mathbf{q}sl}|^2=\hbar\Xi^2q/2Dv_{sl}$,[38] and due to the piezoelectric field with $|M_{\mathbf{q}pl}|^2=(32\hbar\pi^2e^2e_{14}^2/\kappa^2Dv_{sl})[(3q_xq_yq_z)^2/q^7]$ for the longitudinal mode[39] and $\Sigma_{j=1,2}|M_{\mathbf{q}pt_j}|^2=(32\hbar\pi^2e^2e_{14}^2/\kappa^2Dv_{st}q^5)[q_x^2q_y^2+q_y^2q_z^2+q_z^2q_x^2-(3q_xq_yq_z)^2/q^2]$ for the two transverse modes.[40] Here, $\Xi=7$ eV stands for the acoustic deformation potential; $D=5.3\times10^3$ kg/m^3 is the GaAs volume density, $e_{14}=1.41\times10^9$ V/m denotes the piezoelectric constant and the static dielectric constant κ is 12.9, $v_{sl}=5.29\times10^3$ m/s corresponds to the longitudinal sound velocity, and $v_{st}=2.48\times10^3$ m/s corresponds to the transverse one.[41]

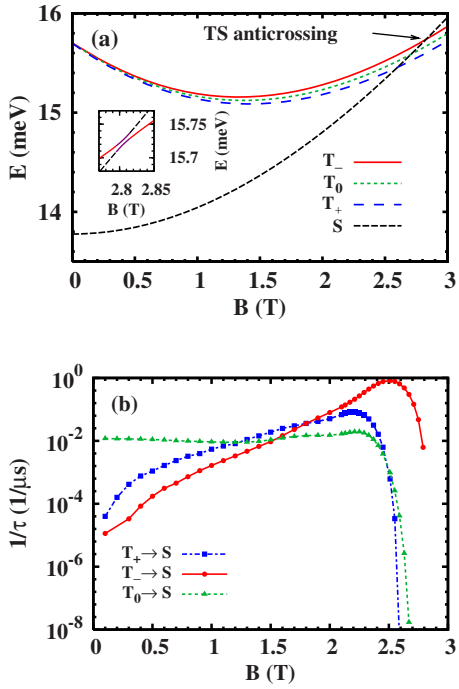

FIG. 1. (Color online) (a) The lowest four energy levels vs magnetic field B in single QD. The TS anticrossing point between T_- and S is shown and the range near this point is enlarged in the inset. (b) τ^{-1} of the three transition channels vs the magnetic field. In the calculation, $d=5$ nm and $d_0=30$ nm.

In our calculation, g factor is -0.44,[4,41] and the Dresselhaus coefficient γ is 21.5 Å^3 eV.[42] The typical electron effective mass m^* in GaAs is $0.067m_0$,[41] with m_0 being the free electron mass.

A. Single dot

We first set $a=0$ to investigate the single dot case by exact diagonalization method with the lowest 800 singlet and 2220 triplet basis functions. Under the basis, the energy levels and the TS relaxation rates are well converged. The magnetic field dependence of the first four levels and that of the TS relaxation rates are plotted in Fig. 1. In the calculation, we take the well width $2d=10$ nm and the effective diameter $d_0=30$ nm. From Fig. 1(a), one notices that the ground state is a singlet denoted as S, in a wide range of the magnetic field (from 0 to 2.6 T approximately). In this region, the first three excited states are triplet states, labeled as $|T_+\rangle$ (spin up), $|T_0\rangle$ (spin zero), and $|T_-\rangle$ (spin down), and the energy of $|T_-\rangle$ is the highest one among the three because of the Zeeman effect. When the magnetic field increases from 2.6 T, one further observes a TS crossing between the singlet and the two triplets ($|T_+\rangle$ and $|T_0\rangle$). Moreover, a TS anticrossing point [with a small energy gap shown in Fig. 1(a)] also exists between the singlet and $|T_-\rangle$ triplet state due to the Dresselhaus spin-orbit coupling. From the calculation, we notice that the major components of $|S\rangle$, $|T_\pm\rangle$, and $|T_0\rangle$ are $|S^1\rangle$, $|T_\pm^1\rangle$,

and $|T_0^1\rangle$, which are the lowest singlet and triplet basis functions. Specifically, using the lowest two single-particle wave functions, $|nln_z\rangle$ with $n=n_z=0$, $l=0$ and -1, one can construct $|S^1\rangle$ with $|000\rangle$ and $|000\rangle$, and $|T_\pm^1\rangle$ and $|T_0^1\rangle$ with $|000\rangle$ and $|0-10\rangle$ according to Eqs. (10)–(13). Therefore, the quantum numbers (L,S_z) of $|S^1\rangle$, $|T_+^1\rangle$, $|T_0^1\rangle$, and $|T_-^1\rangle$ are different, i.e., (0,0), (−1,1), (−1,0), and (−1,−1), respectively.

From Fig. 1(b) one observes that the TS relaxation rates increase slowly with the magnetic field away from the crossing and/or anticrossing points, but decrease dramatically in the vicinity of the crossing and/or anticrossing points, in agreement with the measurement qualitatively.[11] The relaxation rate reaches maximum where the wavelength of the emissive phonon is comparable with the dot size.[43] In our calculation, the TS splitting, i.e., the energy between the triplet and the singlet, $\Delta_{TS}\sim 0.2$ meV. The corresponding half-wavelength of the transverse phonon is therefore about 30 nm as the dot diameter d_0. This feature was interpreted as the competing effects of the magnetic field on the electron-phonon coupling and the spin-orbit coupling.[24] Actually, the strength of the spin-orbit coupling is proportional to α [see Eq. (6)] which increases with the magnetic field,[14] whereas the electron-phonon scattering becomes rather weak when the emissive phonon momentum decreases.[24]

Surprisingly, our results are very different from those shown in the previous work, where the transition rate of $|T_-\rangle$ is much larger than those of the other two triplet states $|T_+\rangle$ and $|T_0\rangle$.[24] In that work, the authors interpreted their results by the selection rule based on the perturbation method including the lowest four basis functions, i.e., $|S^1\rangle$, $|T_+^1\rangle$, $|T_0^1\rangle$, and $|T_-^1\rangle$. Under that basis, only $|T_-\rangle$ is coupled with $|S\rangle$ through the Dresselhaus spin-orbit coupling according to Eq. (15). So only the transition from $|T_-\rangle$ to $|S\rangle$ can occur. Thus they concluded that the transition rate from $|T_-\rangle$ to $|S\rangle$ is much larger than those of the other channels even though much more (instead of four) basis functions are included. In fact, this selection rule is widely used in the literature.[10,11] However, as one needs many basis functions to achieve convergence even in the single-electron QD system,[14] whether the selection rule from the lowest four basis functions is robust against the inclusion of higher basis functions remains an open question. Here we reexamine the selection rule with more basis functions. Assuming the perturbation based on the lowest four states $|S^1\rangle$, $|T_\pm^1\rangle$, and $|T_0^1\rangle$ is adequate to describe the real physics, we expect that the selection rule should always be valid when more basis functions are included. Specifically, we now use four single-electron functions $|000\rangle$, $|0-10\rangle$, $|010\rangle$ and $|0-20\rangle$ to construct the two-electron basis functions. Keeping only the index of l from $|nln_z\rangle$ since the other two are fixed, the six lowest singlet states are constructed by $|0\rangle|0\rangle$, $|0\rangle|-1\rangle$, $|0\rangle\ |1\rangle$, $|-1\rangle|-1\rangle$, $|0\rangle|-2\rangle$, and $|-1\rangle|1\rangle$ separately and the three lowest triplet states are constructed by $|0\rangle|-1\rangle$ in the way of Eqs. (10)–(13). We denote these nine basis functions as $|S^1\rangle$, $|S^2\rangle$, $|S^3\rangle$, $|S^4\rangle$, $|S^5\rangle$, $|S^6\rangle$, $|T_+^1\rangle$, $|T_0^1\rangle$, and $|T_-^1\rangle$ in sequence, and the quantum numbers (L,S_z) are (0,0), (−1,0), (1,0), (−2,0), (−2,0), (0,0), (−1,1), (−1,0), and (−1,−1) respectively. Therefore, only the singlet states $|S^1\rangle$ and $|S^6\rangle$ can mix with $|T_-^1\rangle$; $|S^4\rangle$ and $|S^5\rangle$ can mix with $|T_+^1\rangle$, according to Eq. (15) under these basis functions. No mixing occurs to the state $|T_0^1\rangle$.

As the Coulomb interaction is too strong to treat perturbatively, we first diagonalize the Hamiltonian with the Coulomb interaction included to obtain a set of basis functions, i.e., $|\bar{S}^1\rangle=a_1|S^1\rangle+b_1|S^6\rangle$, $|\bar{S}^2\rangle=a_2|S^1\rangle+b_2|S^6\rangle$, $|\bar{S}^3\rangle=a_3|S^4\rangle+b_3|S^5\rangle$, $|\bar{S}^4\rangle=a_4|S^4\rangle+b_4|S^5\rangle$, $|\bar{S}^5\rangle=|S^2\rangle$, $|\bar{S}^6\rangle=|S^3\rangle$, $|\bar{T}_+^1\rangle=|T_+^1\rangle$, $|\bar{T}_0^1\rangle=|T_0^1\rangle$, and $|\bar{T}_-^1\rangle=|T_-^1\rangle$. Here a_i and b_i are obtained from the numerical diagonalization. The corresponding eigenvalues are E_1 to E_6, E_+, E_0, and E_-, respectively. Then we treat the spin-orbit coupling as perturbation under the basis functions. The lowest four states then read

$$|T_+\rangle = |T_+^1\rangle + \theta_+^1|S^4\rangle + \theta_+^2|S^5\rangle, \tag{17}$$

$$|T_0\rangle = |T_0^1\rangle, \tag{18}$$

$$|T_-\rangle = |T_-^1\rangle + \theta_-^1|S^1\rangle + \theta_-^2|S^6\rangle, \tag{19}$$

$$|S\rangle = \theta_s^1|S^1\rangle + \theta_s^2|S^6\rangle + \theta_s^3|T_-^1\rangle, \tag{20}$$

with $\theta_+^{1(2)}=\Sigma_{i=3,4}\frac{(b_i^*-a_i^*)\mathcal{A}}{E_+-E_i}\Theta_i^{1(2)}$, $\theta_s^{1(2)}=\Theta_1^{1(2)}$, $\theta_-^{1(2)}=\Sigma_{i=1,2}\frac{a_i^*\mathcal{A}+b_i^*\mathcal{B}}{E_--E_i}\Theta_i^{1(2)}$, and $\theta_s^3=\frac{a_1\mathcal{A}+b_1\mathcal{B}}{E_--E_1}$. Here $\Theta_i^{1(2)}=a_i(b_i)$, $\mathcal{A}=-i\gamma^*\alpha(1-eB/2\hbar\alpha^2)$, and $\mathcal{B}=-\frac{i}{\sqrt{2}}\gamma^*\alpha(1+eB/2\hbar\alpha^2)$ with γ^* being $\gamma(\pi/2d)^2$.

Obviously, the transitions from both $|T_+\rangle$ and $|T_-\rangle$ to $|S\rangle$ can occur according to Eqs. (17)–(20). The matrix elements $|\langle f|\chi|i\rangle|^2$ in Eq. (16) now read

$$\begin{aligned}|\langle S|\chi|T_+\rangle|^2 &= |\theta_s^{1*}\theta_+^2\langle S^1|\chi|S^5\rangle + \theta_s^{2*}\theta_+^1\langle S^6|\chi|S^4\rangle|^2 \\ &= (xt)^2|\xi|^2 I^2(q_z),\end{aligned} \tag{21}$$

$$\begin{aligned}|\langle S|\chi|T_-\rangle|^2 &= |\theta_s^{1*}\theta_-^1\langle S^1|\chi|S^1\rangle + \theta_s^{2*}\theta_-^2\langle S^6|\chi|S^6\rangle \\ &\quad + \theta_s^{3*}\langle T_-^1|\chi|T_-^1\rangle|^2 I^2(q_z) = |2t\zeta_1 - tx\zeta_2|^2 I^2(q_z),\end{aligned} \tag{22}$$

with $x=k_\parallel^2/4\alpha^2$, $t=e^{-x}$, $I(q_z)=\pi^2\sin(dq_z)/\{dq_z[\pi^2-(dq_z)^2]\}$, $\zeta_1=\theta_s^{3*}+\theta_s^{1*}\theta_-^1+\theta_s^{2*}\theta_-^2$, $\zeta_2=\theta_s^{3*}+2\theta_s^{2*}\theta_-^2$, and $\xi=\theta_s^{1*}\theta_+^2+\sqrt{2}\theta_s^{2*}\theta_+^1$. We calculate the relaxation rates of these two channels and plot the results in Fig. 2. One notices that the two sets of dots (▲ for $|T_+\rangle$ and ● for $|T_-\rangle$) are quite close to each other and even show a crossing. In other words, the selection rule is violated. We also present the exact diagonalization results under the same basis functions $|S^1\rangle-|S^6\rangle$, $|T_0^1\rangle$, and $|T_\pm^1\rangle$ in Fig. 2 (dashed curve for $|T_+\rangle$ and solid curve for $|T_-\rangle$). It is seen that the diagonalization results almost exactly match the perturbation results. This match further confirms that both our exact diagonalization and the perturbation calculations are correct. Compare Fig. 2 with Fig. 1(b), it is obvious that the high excited levels manifest themselves markedly in the relaxation rates. From our calculation, we notice that the coefficients in Eqs. (17) and (19) are comparable. This is because the denominators E_--E_i in $\theta_-^{1(2)}$ are close to E_+-E_i in $\theta_+^{1(2)}$. This explains the reason why the curve of $|T_-\rangle$ is close to that of $|T_+\rangle$ in Fig. 2.

However, it is noted that the selection rule works well in the vicinity of the crossing and/or anticrossing points both in

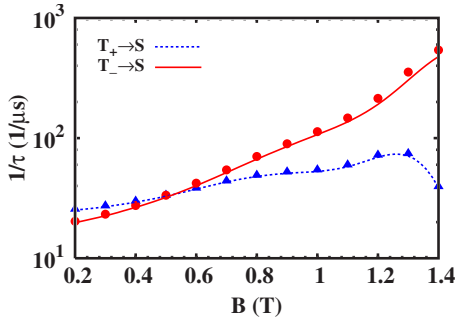

FIG. 2. (Color online) Comparison of the TS relaxation rates of T_- and T_+ in single QD calculated from the perturbation method and the exact diagonalization method limited within nine basis functions ($|S^1\rangle$ to $|S^6\rangle$, $|T^1_\pm\rangle$, and $|T^1_0\rangle$). Dashed curve and ▲: $1/\tau_{T_+\to S}$ from the exact diagonalization and perturbation methods respectively; solid curve and ●: $1/\tau_{T_-\to S}$ from the exact diagonalization and perturbation methods.

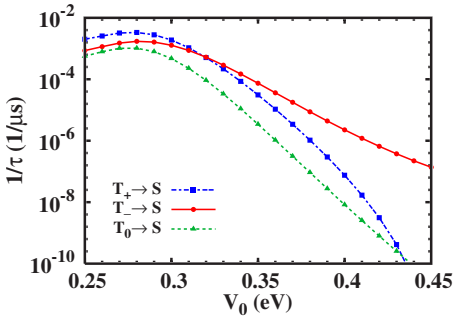

FIG. 3. (Color online) τ^{-1} vs barrier height in double QDs. In the calculation, $a=8$ nm, $d=7$ nm, $d_0=30$ nm, and $B=0.5$ T.

Figs. 1(b) and 2.[44] This can be understood from Eqs. (17) and (19). Near the TS crossing point where $E_+\sim E_1$, the energy splitting $E_+-E_{3,4}$ is finite. Therefore $\theta_+^{1(2)}$ only changes slightly compared with the region away from the TS crossing. Similar is true for the coefficients of $|T_0\rangle$. In contrast, $\theta_-^{1(2)}$ is very large when $E_-\sim E_1$. Therefore the transition rate from $|T_-\rangle$ would be much larger than those from $|T_+\rangle$ and $|T_0\rangle$, i.e., the selection rule is valid in the vicinity of the TS crossing and/or anticrossing point. Moreover, the effect of the Zeeman splitting also makes the transition rate of $|T_-\rangle$ larger than those of $|T_+\rangle$ and $|T_0\rangle$ because of the larger phonon momentum q. Specifically, the energy splitting between $|T_-\rangle$ and $|S\rangle$ is about 0.18 meV at $B=2.5$ T in Fig. 1(a), which is much larger than that between $|T_+\rangle$ ($|T_0\rangle$) and $|S\rangle$, i.e., ~0.06 meV (0.12 meV). As the transition rates are proportional to q^m with $m>0$ varying for different mechanisms, the rate of $|T_-\rangle$ is much larger than those of $|T_+\rangle$ and $|T_0\rangle$.

B. Double dot

Now we turn to study the TS relaxation rate in weakly coupled double QDs using basis functions including 400 singlet and 1080 triplet states. In the calculation, $a=8$ nm and $d=7$ nm. In this part we still use $|T_\pm\rangle$ and $|T_0\rangle$ ($|S\rangle$) to denote eigenfunctions of the lowest three triplet states (lowest singlet state). To determine the contribution of the energy levels along the z axis, we take the barrier height $V_0=0.25$ meV, the lowest one in our calculation, as an example. In this configuration the splitting between the first and the second levels along the z axis is about 1 meV and that between the second and the third levels is much larger, about 0.2 eV. Compared with the lateral confinement (~4 meV for $d_0=30$ nm), we only need to include the lowest two in our calculation.

We first investigate the TS relaxation rate as a function of the barrier height. In the calculation, $d_0=30$ nm and $B=0.5$ T. As shown in Fig. 3, each transition rate first increases slowly until it reaches the maximum around $V_0\sim 0.28$ eV where the TS splitting $\Delta_{TS}\sim 0.4$ meV corresponding to the wavelength of the emissive phonon being comparable with the dot size d_0.[43] After that, the TS relaxation rate decreases rapidly with the barrier height. This would offer us a scheme to manipulate the TS relaxation in double QDs. Similar features (not shown here) are obtained when we increase the interdot distance. The dramatic decrease of the relaxation rate can be understood as follows. When the barrier height becomes higher or the interdot distance becomes larger, the interdot coupling is weakened and the energy splitting between the lowest two levels along the z axis becomes smaller. As a result, the splitting between $|T_\pm\rangle$ ($|T_0\rangle$) and $|S\rangle$ decreases too. This causes the decrease of the TS relaxation rate as discussed in the previous subsection.

To have a look at the role of the magnetic field, we calculate the average relaxation rate $1/\bar{\tau}=(1/\tau_{T_+\to S}+1/\tau_{T_-\to S}+1/\tau_{T_0\to S})/3$ as function of the barrier height at different magnetic fields in Fig. 4(a), but with the dot size $d_0=30$ nm fixed. It is seen from the figure that higher magnetic field leads to relatively larger transition rate. It is due to the enhanced spin-orbit coupling in strong magnetic field. The influence of the effective diameter of QDs with $V_0=0.35$ V and $B=1$ T is also shown in Fig. 4(b). One finds the transition rates increase with the effective diameter d_0. The reason lies on the different symmetry properties of the singlet and triplet states. For the singlet state, the interelectron distance decreases with the decrease of the dot size. The Coulomb repulsion therefore lifts the corresponding energy levels.

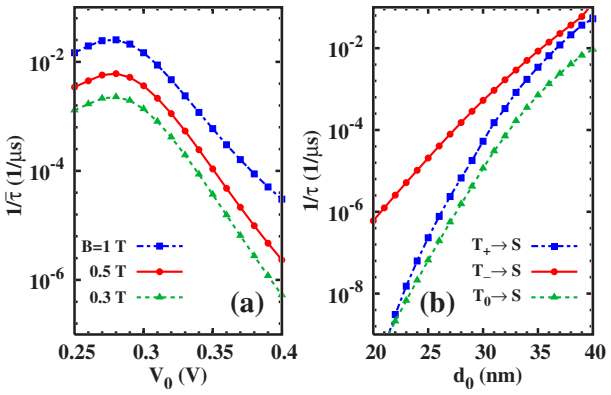

FIG. 4. (Color online) (a) Average TS relaxation rate $\bar{\tau}^{-1}$ vs barrier height at different magnetic fields in double QDs. In the calculation, $a=8$ nm, $d=7$ nm, and $d_0=30$ nm. (b) τ^{-1} vs effective dot diameter. In the calculation, $a=8$ nm, $d=7$ nm, $V_0=0.35$ V, and $B=1$ T.

However, the energy lifts of the triplet states are smaller due to the antisymmetry property of the triplet states which prevents the electrons to be close to each other. Therefore, the TS splitting becomes smaller with the decrease of the dot size. This leads to the rapid decrease of the TS relaxation rates.

IV. SUMMARY

In summary, we have investigated the TS relaxation in single and double QDs. For the single dot case, we find that the average relaxation rate first slowly increases with magnetic field until it reaches the maximum where the wavelength of emissive phonon is comparable with the dot size. Then it drops sharply. This result qualitatively agrees with the recent measurement.[11] Furthermore, our result shows the transition rates of the triplet $|T_+\rangle$ and $|T_0\rangle$ can be comparable with that of $|T_-\rangle$, which violates the selection rule in the literature.[24] We show that the selection rule obtained from the lowest four basis functions does not hold in general cases where much more basis functions are needed to converge the triplet and/or singlet states. This is shown perturbatively by calculating the TS relaxation rates based on nine basis functions. Comparable transition rates of $|T_+\rangle$ and $|T_-\rangle$ are immediately obtained away from the TS crossing point. The perturbation results are in good agreement with the exact diagonalization results under the same basis functions. We also show that the selection rule works well in the vicinity of the TS crossing and/or anticrossing point due to the effects from the Zeeman splitting and the anticrossing. For the double QD case, we demonstrate that the TS relaxation rates vary more than 2 orders of magnitude by tuning the interdot barrier. This offers a feasible scheme to manipulate the TS relaxation in double QDs. The relaxation rates also sensitively depend on the dot size and magnetic field.

ACKNOWLEDGMENTS

This work was supported by the Natural Science Foundation of China under Grant Nos. 10574120 and 10725417, the National Basic Research Program of China under Grant No. 2006CB922005, the Knowledge Innovation Project of Chinese Academy of Sciences, and SRFDP.

APPENDIX: Q IN COULOMB INTERACTION

Following Ref. 14, we obtain Q in Eq. (14) as

$$Q(N_1,N_2,N_1',N_2') = \int_0^\infty dk_\parallel k_\parallel P_{N_1,N_1'}(k_\parallel) P_{N_2',N_2}(k_\parallel) \int_{-\infty}^\infty dk_z \times \frac{W_{N_1,N_1'}(k_z) W^*_{N_2',N_2}(k_z)}{k^2}, \tag{A1}$$

where $P_{N,N'}$ and $W_{N,N'}$ come from the lateral and vertical parts of the matrix element $\langle n,l,n_z|\exp(i\mathbf{k}\cdot\mathbf{r})|n',l',n_z'\rangle$, respectively. P is given by[14]

$$P_{N,N'}(k_\parallel) = \sqrt{\frac{n!n'!}{(n+|l|)!(n'+|l'|)!}} \exp\left(-\frac{k_\parallel^2}{4\alpha^2}\right) \times \sum_{i=0}^{n'} \sum_{j=0}^{n} C^i_{n',|l'|} C^j_{n,|l|} \bar{n}! L_{\bar{n}}^{|l-l'|}\left(\frac{k_\parallel^2}{4\alpha^2}\right) \times \left[\mathrm{sgn}(l'-l)\frac{k_\parallel}{2\alpha}\right]^{|l'-l|}, \tag{A2}$$

with $C^i_{n,l} = \frac{(-1)^i}{i!}\binom{n+l}{n-i}$ and $\bar{n} = i+j+(|l|+|l'|-|l'-l|)/2$. sgn (x) represents the sign function. W reads

$$W_{N,N'} = \langle n_z|\exp(ik_z z)|n_z'\rangle. \tag{A3}$$

*Author to whom correspondence should be addressed; mwwu@ustc.edu.cn
†Mailing address.

[1] D. Loss and D. P. DiVincenzo, Phys. Rev. A **57**, 120 (1998).
[2] R. Hanson, L. P. Kouwenhoven, J. R. Petta, S. Tarucha, and L. M. K. Vandersypen, Rev. Mod. Phys. **79**, 1217 (2007).
[3] *Semiconductor Spintronics and Quantum Computation*, edited by D. D. Awschalom, D. Loss, and N. Samarth (Springer-Verlag, Berlin, 2002); I. Zutić, J. Fabian, and S. Das Sarma, Rev. Mod. Phys. **76**, 323 (2004), and references therein.
[4] R. Hanson, B. Witkamp, L. M. K. Vandersypen, L. H. Willems van Beveren, J. M. Elzerman, and L. P. Kouwenhoven, Phys. Rev. Lett. **91**, 196802 (2003).
[5] S. Amasha, K. Maclean, Iuliana Radu, D. M. Zumbühl, M. A. Kastner, M. P. Hanson, and A. C. Gossard, arXiv:cond-mat/0607110 (unpublished).
[6] F. H. L. Koppens, C. Buizert, K. J. Tielrooij, I. T. Vink, K. C. Nowack, T. Meunier, L. P. Kouwenhoven, and L. M. K. Vandersypen, Nature (London) **442**, 766 (2006).
[7] J. R. Petta, A. C. Johnson, J. M. Taylor, E. A. Laird, A. Yacoby, M. D. Lukin, C. M. Marcus, M. P. Hanson, and A. C. Gossard, Science **309**, 2180 (2005).
[8] F. H. L. Koppens, J. A. Folk, J. M. Elzerman, R. Hanson, L. H. Willems van Beveren, I. T. Vink, H. P. Tranitz, W. Wegscheider, L. P. Kouwenhoven, and L. M. K. Vandersypen, Science **309**, 1346 (2005).
[9] J. R. Petta, A. C. Johnson, A. Yacoby, C. M. Marcus, M. P. Hanson, and A. C. Gossard, Phys. Rev. B **72**, 161301(R) (2005).
[10] S. Sasaki, T. Fujisawa, T. Hayashi, and Y. Hirayama, Phys. Rev. Lett. **95**, 056803 (2005).
[11] T. Meunier, I. T. Vink, L. H. Willems van Beveren, K.-J. Tielrooij, R. Hanson, F. H. L. Koppens, H. P. Tranitz, W. Wegscheider, L. P. Kouwenhoven, and L. M. K. Vandersypen, Phys. Rev. Lett. **98**, 126601 (2007).
[12] L. M. Woods, T. L. Reinecke, and Y. Lyanda-Geller, Phys. Rev. B **66**, 161318(R) (2002).
[13] R. de Sousa and S. Das Sarma, Phys. Rev. B **68**, 155330 (2003).
[14] J. L. Cheng, M. W. Wu, and C. Lü, Phys. Rev. B **69**, 115318 (2004).
[15] D. V. Bulaev and D. Loss, Phys. Rev. B **71**, 205324 (2005).

[16] V. N. Golovach, A. Khaetskii, and D. Loss, Phys. Rev. Lett. **93**, 016601 (2004).
[17] C. F. Destefani and S. E. Ulloa, Phys. Rev. B **72**, 115326 (2005).
[18] P. San-Jose, G. Zarand, A. Shnirman, and G. Schön, Phys. Rev. Lett. **97**, 076803 (2006).
[19] V. I. Fal'ko, B. L. Altshuler, and O. Tsyplyatev, Phys. Rev. Lett. **95**, 076603 (2005).
[20] Y. Y. Wang and M. W. Wu, Phys. Rev. B **74**, 165312 (2006).
[21] P. Stano and J. Fabian, Phys. Rev. Lett. **96**, 186602 (2006).
[22] P. Stano and J. Fabian, Phys. Rev. B **74**, 045320 (2006).
[23] H. Westfahl, Jr., A. O. Caldeira, G. Medeiros-Ribeiro, and M. Cerro, Phys. Rev. B **70**, 195320 (2004).
[24] J. I. Climente, A. Bertoni, G. Goldoni, M. Rontani, and E. Molinari, Phys. Rev. B **75**, 081303(R) (2007).
[25] V. N. Golovach, A. Khaetskii, and D. Loss, arXiv:cond-mat/0703427 (unpublished).
[26] J. I. Climente, A. Bertoni, G. Goldoni, M. Rontani, and E. Molinari, Phys. Rev. B **76**, 085305 (2007).
[27] M. Florescu and P. Hawrylak, Phys. Rev. B **73**, 045304 (2006).
[28] G. Dresselhaus, Phys. Rev. **100**, 580 (1955).
[29] E. I. Rashba, Fiz. Tverd. Tela (Leningrad) **2**, 1224 (1960).
[30] D. Paget, G. Lample, B. Sapoval, and V. I. Safarov, Phys. Rev. B **15**, 5780 (1977).
[31] G. E. Pikus and A. N. Titkov, *Optical Orientation* (Berlin, Springer, 1984).
[32] Sigurdur I. Erlingsson, Yuli V. Nazarov, and Vladimir I. Fal'ko, Phys. Rev. B **64**, 195306 (2001).
[33] V. Fock, Z. Phys. **47**, 446 (1928).
[34] C. G. Darwin, Proc. Cambridge Philos. Soc. **27**, 86 (1930).
[35] D. G. Austing, S. Sasaki, K. Muraki, K. Ono, S. Tarucha, M. Barranco, A. Emperador, M. Pi, and F. Garcias, Int. J. Quantum Chem. **91**, 498 (2003).
[36] W. H. Lau and M. E. Flatté, Phys. Rev. B **72**, 161311(R) (2005).
[37] M. I. D'yakonov and V. I. Perel', Zh. Eksp. Teor. Fiz. **60**, 1954 (1971) [Sov. Phys. JETP **38**, 1053 (1971)].
[38] P. Vogl, *Physics of Nonlinear Transport in Semiconductors*, Nato Advanced Study Institute Series B52, edited by D. K. Ferry, J. R. Barker, and C. Jacoboni (Plenum, New York, 1980).
[39] G. D. Mahan, *Polarons in Ionic Crystals and Polar Semiconductors*, edited by J. T. Devreese (North-Holland, Amsterdam, 1972).
[40] X. L. Lei, J. L. Birman, and C. S. Ting, J. Appl. Phys. **58**, 2270 (1985).
[41] *Semiconductors*, Landolt-Börnstein, New Series, Vol. 17a, edited by O. Madelung (Springer-Verlag, Berlin, 1987).
[42] D. Richards, B. Jusserand, H. Peric, and B. Etienne, Phys. Rev. B **47**, 16028 (1993).
[43] U. Bockelmann and G. Bastard, Phys. Rev. B **42**, 8947 (1990).
[44] Under the basis for Fig. 2, the TS crossing and/or anticrossing occurs near $B=1.6$ T (not shown). Therefore, the selection rule already works at $B>1.3$ T.